Chemical Physics Letters 746 (2020) 137302

Contents lists available at ScienceDirect

Chemical Physics Letters

journal homepage: www.elsevier.com/locate/cplett

Research paper

Photocatalytic degradation of methyl orange dye under UV irradiation in the presence of synthesized PVP capped pure and gadolinium doped ZnO nanoparticles

Rupy Dhir

Department of Chemistry G.S.S.D.G.S. Khalsa College, Patiala, Punjab, India

HIGHLIGHTS

- Synthesis of $Zn_{1-x}Gd_xO$ nanoparticles using wet chemical co-precipitation technique.
- Polyvinylpyrrolidne was used as a capping agent.
- The synthesized nanoparticles were used as photocatalysts for the degradation of methyl orange dye.
- Doping of ZnO nanoparticles has greatly increased its catalytic efficiency.

ARTICLE INFO

Keywords:
Nanophotocatalysts
Chemical co-precipitation
Doping

ABSTRACT

The present study focuses on the development of efficient nanophotocatalysts (pure and Gadolinium doped Zinc oxide) for the degradation of methyl orange dye in polluted water. Chemical co-precipitation technique was employed for the synthesis of target compounds using zinc acetate and gadolinium nitrate as metal precursors. The synthesized nanoparticles were characterized by various spectroscopic techniques namely X-ray diffraction, Fourier Transform infra red spectroscopy, Field emission scanning electron microscopy and energy dispersive X-ray spectroscopy. The synthesized pure and Gadolinium doped Zinc oxide nanoparticles were used as photocatalysts for the degradation of methyl orange dye under ultra-violet light irradiation. Doping of ZnO nanoparticles with Gadolinium has greatly increased its catalytic efficiency.

1. Introduction

Water pollution is one of the major environmental challenges, humankind is facing these days. The dyes which are widely used in textile, plastic, medicine and many other industries are the main cause of water pollution [1]. Azo dyes such as methyl orange constitutes about half of textile dyes [2]. The presence of these dyes in water sources contribute to toxicity, eutrophication and hinder the infiltration of sunlight, thus severely affect the growth of aquatic life [3] and causing long-term health effects [4]. Current methods including conventional sewage plant treatment [5] do not degrade harmful chemicals present in dyes and only insufficiently remove them from polluted water. An alternative and highly efficient technique for the degradation of dye is photocatalysis using semiconductor photocatalysts [6–9]. The photocatalysts are the substances that chemically react with dyes in the presence of light and convert them into non toxic products by oxidation process. Comparing the photocatalytic activity of various semiconductor photocatalysts in aqueous media, zinc oxide (ZnO) is found to be on top position [10,11] and its photocatalytic activity can be further enhanced by moving from bulk to nano ZnO. [12]. It is because of large surface area of nanomaterials thus produces large number of active sites. Doping of ZnO nanomaterials further increases its photocatalytic efficiency towards the degradation of dyes [13–23]. Literature study has revealed that doping of ZnO nanoparticles with rare earth metal atoms have significantly increased its photocatalytic efficiency towards the degradation of organic dyes in water [24–30]. Doping introduces another metal ions by substituting Zn ions from their original lattice points and produces traps photogenerated charge carriers which inturn lower the electron hole pair recombination rate, hence increases the photocatalytic efficiency.

To best of my knowledge, studies on the photocatalytic degradation of methyl orange dye using Gadolinium doped (Gd-doped) ZnO nanoparticles are scarce in literature. So, in the present investigation, Gd-doped ZnO nanoparticles were synthesized by chemical co-precipitation method using zinc acetate and gadolinium nitrate as metal precursors. The synthesized nanoparticles were characterized by various

E-mail address: rupydhir431@yahoo.com.

https://doi.org/10.1016/j.cplett.2020.137302
Received 15 December 2019; Received in revised form 1 February 2020; Accepted 2 March 2020
Available online 08 March 2020
0009-2614/

spectroscopic techniques namely X-ray diffraction (XRD), Fourier Transform infra red spectroscopy (FT-IR), Field emission scanning electron microscopy (FESEM), energy dispersive X-ray spectroscopy (EDXRF) and optical studies. (PC) degradation of methyl orange dye was studied in aqueous medium in the presence of synthesized nanoparticles under the irradiation of UV light.

2. Experimental procedure

2.1. Materials

Gadolinium (III) nitrate hexahydrate (99.9%) was purchased from Sigma Aldrich. Co, 3050, St. Louis, MO, USA, Zinc acetate, sodium hydroxide, polyvinyl pyrrolidone and methyl orange were of analytical reagent grade and used without further purification. All solutions used in the experiments were prepared by using triply distilled deionised water.

2.2. Synthesis of $Zn_{1-x}Gd_xO$ nanoparticles

Pure and gadolinium doped ZnO nanoparticles ($Zn_{1-x}Gd_xO$, $0.00001 \leq x \leq 0.1$) were prepared using bottom up wet chemical co-precipitation technique in the presence of polyvinyl pyrrolidone (PVP) as a capping agent. Synthesis was carried out under ambient conditions. In the typical synthetic procedure, stoichiometric proportion of 0.5 M zinc acetate was taken in a titration flask followed by drop wise addition of gadolinium nitrate solution. After stirring the mixture for 1 h, 8 ml. of 2% PVP was added and then 0.5 M sodium hydroxide solution was added drop wise with continuous stirring. Resulting white precipitates were filtered, thoroughly washed and then dried in hot air oven at 150 °C temperature for one hour followed by crushing using mortar and pestle to obtain nanoparticles in fine powder form. The amount of precursors solution used for preparation of Gd-doped ZnO samples is listed in Table 1. Eq. (1) and (2) represents the stepwise formation of ZnO nanoparticles.

$$Zn(CH_3COO)_2(aq.) + 2NaOH(aq.) + \overset{PVP}{\rightarrow} Zn(OH)_2(s) + 2CH_3COONa(aq.) \quad (1)$$

$$Zn(OH)_2(s) \overset{Heat}{\rightarrow} ZnO + H_2O \quad (2)$$

2.3. Characterization

The synthesized Gd-doped ZnO nanoparticles have been characterized using X-ray diffraction, FE scanning electron microscopy, Fourier Transform infrared spectroscopy and energy dispersive x-ray fluorescence techniques. X-ray diffraction spectrum is obtained from powder X-ray diffraction (PAN-Analytic) setup using 3050/60 goniometer and Cu anode X-ray tube. The X- ray diffraction scans were performed in the 2θ range 20–80° keeping step size 0.001for the Cu K X-ray radiation (λ = 1.5406 Å) at 40 mA–45 kV generator setting for the powder samples. For average particle size determination FE scanning electron microscopic micrographs at an accelerating voltage of 5 kV with magnification of 70,000 were taken using Hitachi (SU8000) FE scanning electron microscope. The energy dispersive x-ray fluorescence technique is used for elemental and compositional analysis of synthesized nanomaterials. Energy dispersive x-ray fluorescence spectrometer involving Mo anode X-ray tube (PAN-Analytic) as an excitation source and LEGe (Canberra made, FWHM = 150 eV at 5.89 keV) as photon detector is used to record spectra of the Gd doped ZnO nanomaterials. Fourier Transform Infrared studies were performed using Bruker alfa Fourier Transform Infrared spectrometer.

Table 1
Amount of precursors used in sample preparation.

Sample details $Zn_{1-x}Gd_xO$	Amounts of precursors used in sample preparation		
	Volume of 0.5 M Zn $(OCOCH_3)_2$ solution (ml)	Volume of 0.5 M NaOH solution (ml)	Volume of Gd $(NO_3)_3{\cdot}6H_2O$ (M) solution (ml)
$x = 0.1$	45	50	1.04 (1 M)
$x = 0.01$	49.5	25	1.04 (0.1 M)
$x = 0.001$	49.95	25	1.04 (0.01 M)
$x = 0.0001$	49.995	25	1.04 (0.001 M)
$x = 0.00001$	49.9995	25	1.04 (0.0001 M)
$x = 0.0$	50	25	–

2.4. Photocatalytic behaviour

The photocatalytic behaviour of pure ZnO and Gd-doped ZnO nanomaterials were studied under UV light exposure for the degradation of methyl orange dye in aqueous medium using UV-photoreactor [dimension of 1 ft (height) × 0.5 ft (length)] equipped with one 160 W UV-bulb (OSRAM made 468). The distance between the reactor setup and UV-tube was ~10 cm. 100 mg nanopowder mixed with 250 ml of 16 ppm methyl orange dye solution in a glass reactor with surface area 50 cm^2 was used for photocatalytic studies. For first one hour the above solution was put under constant stirring in dark for the adsorption of dye molecules on the surface of nanoparticles. It was then exposed to the ultraviolet-radiation with continuous magnetic stirring. 10 ml of suspension solution was sampled and centrifuged at fixed time intervals. After centrifugation, the supernatant was analyzed using the ultraviolet–visible spectrophotometer. The concentration of dye was measured from the optical absorption values at a certain wavelength. The equation (3) represents the degradation efficiency (ε) of dye

$$\in = \frac{Co - C}{Co} \times 100 \quad (3)$$

where as C_o and C represent the initial concentration of the dye the concentration after UV irradiation respectively. Furthermore, in accordance to the Langmuir–Hinshelwood kinetics model [31], the photocatalytic process of methyl orange dye can be expressed as apparent pseudo-first-order kinetic Eq. (4).

$$ln\frac{Co}{C} = \kappa t \quad (4)$$

where κ is the apparent pseudo-first-order rate constant, C_o is original methylene blue concentration and C is methylene blue concentration in aqueous solution at time t.

3. Results and discussion

3.1. Crystallographic characterization

Fig. 1a represents the XRD patterns of all the synthesized pure and gadolinium doped ZnO nanoparticles ($Zn_{1-x}Gd_xO$, $0.00001 \leq x \leq 0.1$). The successful synthesis, crystalline nature and hexagonal wurtzite structure of ZnO nanoparticles is confirmed from various sharp peaks in XRD graph observed at 2θ of 31.76°, 34.39, 36.22, 47.52, 56.54, 62.81, and 67.84 correspond to lattice planes (1 0 0), (0 0 2), (1 0 1), (1 0 2), (1 1 0), (1 0 3) and (1 1 2) respectively as reported in JCPDS file no. 05-0664 [32]. The lattice parameters 'a' and 'c' identified by JCPDS for hexagonal wurtzite ZnO are 3.2498 Å and 5.2066 Å respectively. Any diffraction peak related to impurity phase is not detected which indicates the successful substitution of Gd^{3+} ions into Zn^{2+} sites without disturbing wurtzite crystal structure of ZnO. The shifting of peaks shown in Fig. 1b indicates the substitution of Gd in the crystalline ZnO structure. This is due to the expansion of ZnO lattice upon doping with Gadolinium as the ionic radii of Gd^{3+} (0.94 Å) is larger than that of Zn^{2+} (0.74 Å).

Scherrer'r formula [33] Eq. (5), by estimating full width at half

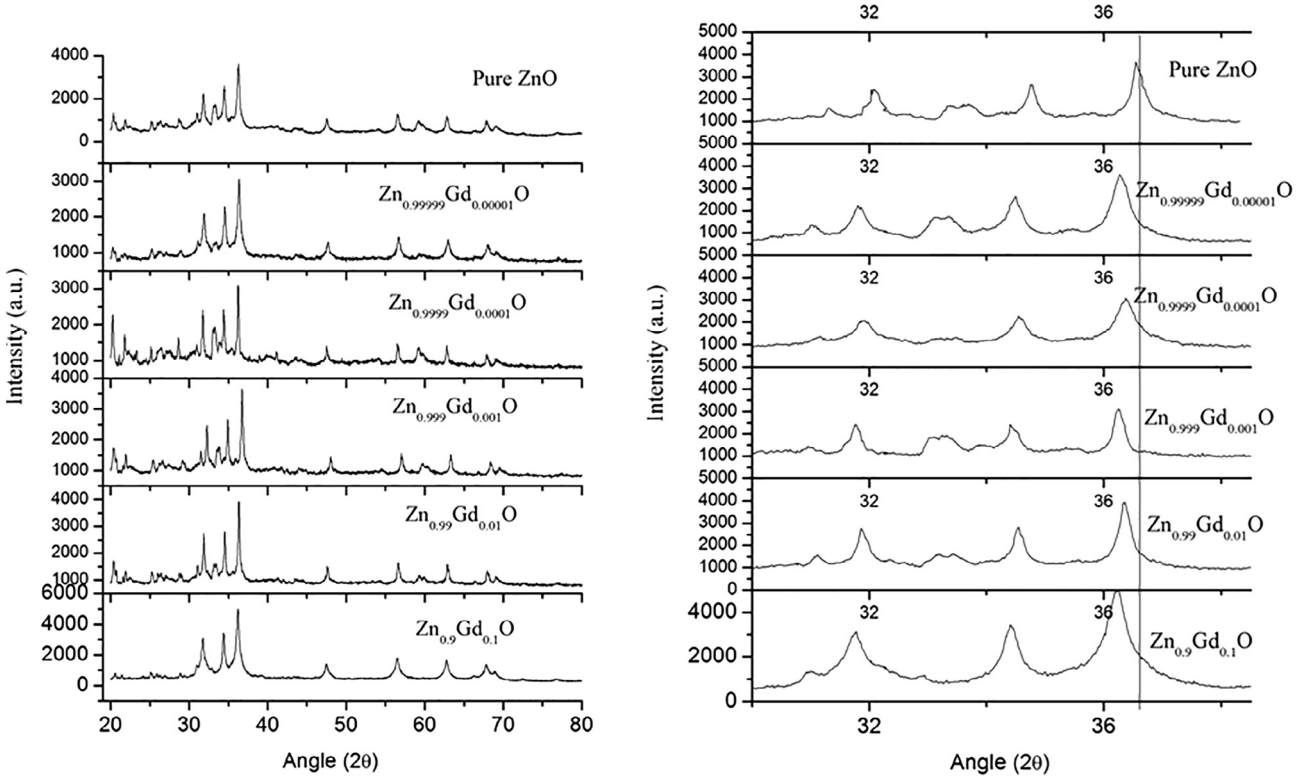

Fig. 1. X- ray diffraction spectra of PVP capped ZnO and $Zn_{1-x}Gd_xO$ ($0.00001 \leq x \leq 0.1$) nanoparticles (a) Angle (2θ) ranges from 20 to 80 (b) Angle (2θ) ranges from 30 to 38.

maximum (FWHM) of sharp peak (1 0 1), was used to calculate the average crystalline size of the prepared nanoparticles.

$$D = \frac{0.89\lambda}{\beta\cos\theta} \quad (5)$$

where λ represents the wavelength of Cu K α radiation, β represents the diffraction peak's full width half maxima, and θ is the Bragg peak angle. The estimated crystalline sizes of $Zn_{1-x}Gd_xO$ ($0.000001 \leq x \leq 0.1$) nanoparticles at most intense crystallographic plane [1 1 0] are found 11.49 nm, 37.94 nm, 41.05 nm, 52.67 nm, 20.38 nm and 18.62 nm for × = 0.10000, 0.01000, 0.00100, 0.00010, 0.00001 and 0.00000 respectively.

3.2. Fourier Transform infrared (FTIR) spectroscopic studies

Fig. 2 represents FTIR spectra of pure and Gd-doped ZnO nanoparticles. The peaks observed at 3471 and 1396 cm^{-1} are assigned to O-H stretching and deformation respectively and is attributed to water adsorption on the metal surface. Due to inter-atomic vibrations, metal oxides generally exhibit absorption bands in fingerprint region i.e. below 1000 cm^{-1}. The peak at 668 is corresponded to Zn-O stretching vibration, which is in accordance with literature values [34]. Various absorption peaks between 900 and 2900 cm^{-1} are also recorded in all samples. Absorption peaks around 900–1020 cm^{-1}, 1300–1600 cm^{-1} and 2850–2950 cm^{-1} are assigned to C–C stretching mode, C–O stretching modes (symmetric and asymmetric) and C–H bond of the acetate group respectively. The above observation and discussion indicates the presence of hydroxy and acetate groups on the surface of pure and Gd-doped ZnO nanoparticles.

3.3. Energy dispersive X-ray fluorescence (EDXRF) studies

Fig. 3a-3d represent the chemical compositions of the prepared pure and gadolinium doped ZnO nanoparticles ($Zn_{1-x}Gd_xO$,

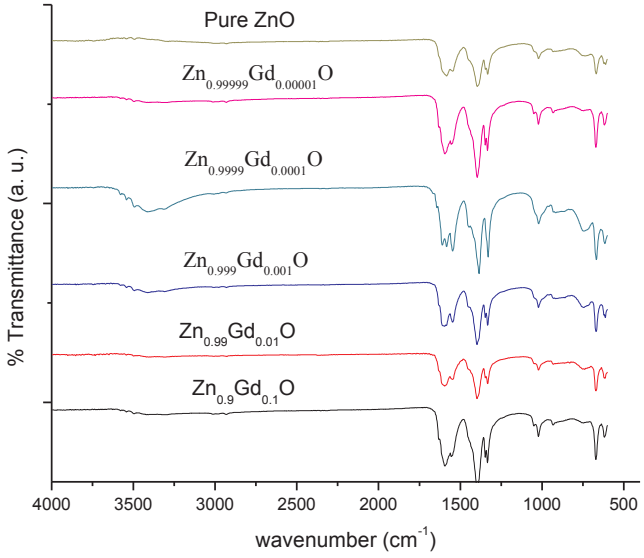

Fig. 2. Fourier Transform Infrared spectra of polyvinyl pyrrolidone capped $Zn_{1-x}Gd_xO$ (x = 0, 0.000001, 0.00001, 0.0001, 0.001, 0.01 and 0.1) nanocrystals.

$0.001 \leq x \leq 0.1$) measured by EDS spectra. From the spectra 3a-3c, the presence of Zn, O and Gd is confirmed in Gd doped ZnO NPs whereas the spectrum 3d of pure ZnO NPs confirmed the presence of only zinc and oxygen ions. The obtained EDS result confirms the doping of ZnO matrix with Gd. The percentage amount of Gd calculated from EDS studies in $Zn_{1-x}Gd_xO$ samples is 1.02, 0.18 and 0.05 against theoretical value of 1, 0.1 and 0.01 for × = 0.01, 0.001 and 0.0001 respectively. The experimental values are in good agreement with the calculated values.

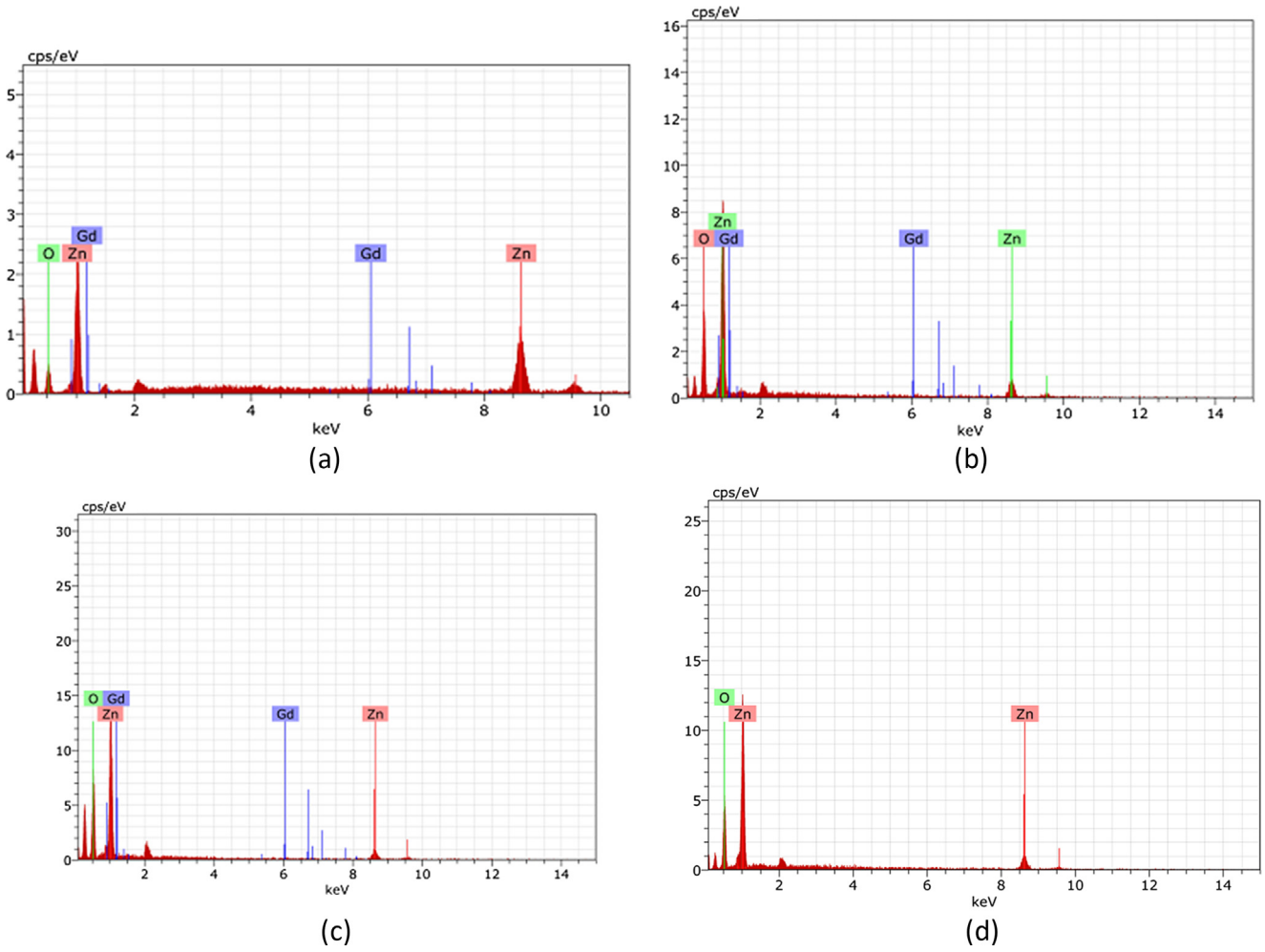

Fig. 3. Energy dispersive x-ray fluorescence spectra of $Zn_{1-x}Gd_xO$ nanocrystals. (a) x = 0.01, (b) x = 0.001, (c) x = 0.0001, (d) x = 0.

3.4. FE scanning electron microscopic studies

The surface morphology of the PVP capped pure and Gd-doped ZnO nanoparticles were examined with FE scanning electron microscope. FE-SEM micrographs of pure ZnO Fig. 4a and $Zn_{0.9}Gd_{0.1}O$ Fig. 4b nanoparticles show spherical clusters of particles. However, the doping with gadolinium results in a decrease in size of clusters.

3.5. Optical studies

Fig. 5 presents the UV–Visible absorption spectra for pure and Gd-doped ZnO nanoparticles. A small shift to longer wavelength (red shift) was observed in the absorption edges upon doping with Gadolinium. Furthermore, the shift in wavelength is directly related to the size of nanoparticles as calculated from XRD data. The absorption edges of $Zn_{1-x}Gd_xO$ ($0.000001 \leq x \leq 0.1$) nanoparticles are 367 nm, 369 nm, 369 nm, 370 nm, 367 nm and 366 nm for × = 0.10000, 0.01000,

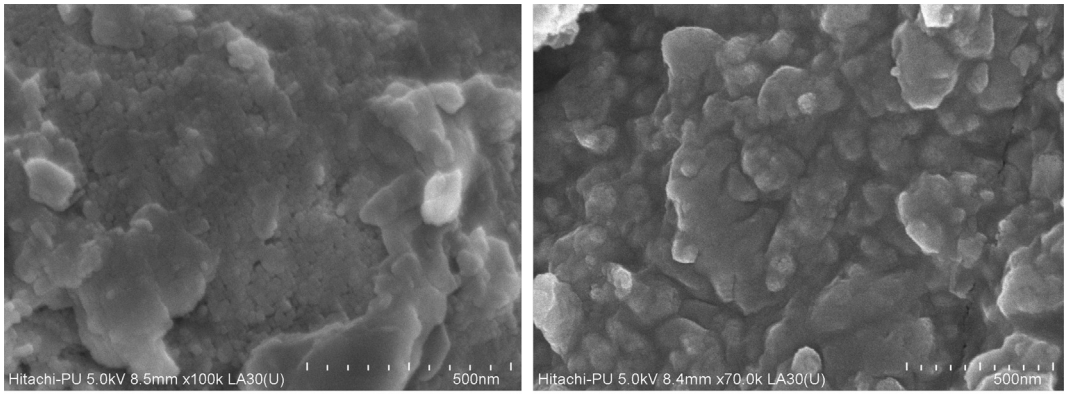

Fig. 4. FE-Scanning electron microscopic micrographs of (a) $Zn_{0.9}Gd_{0.1}O$ and (b) ZnO nanocrystals.

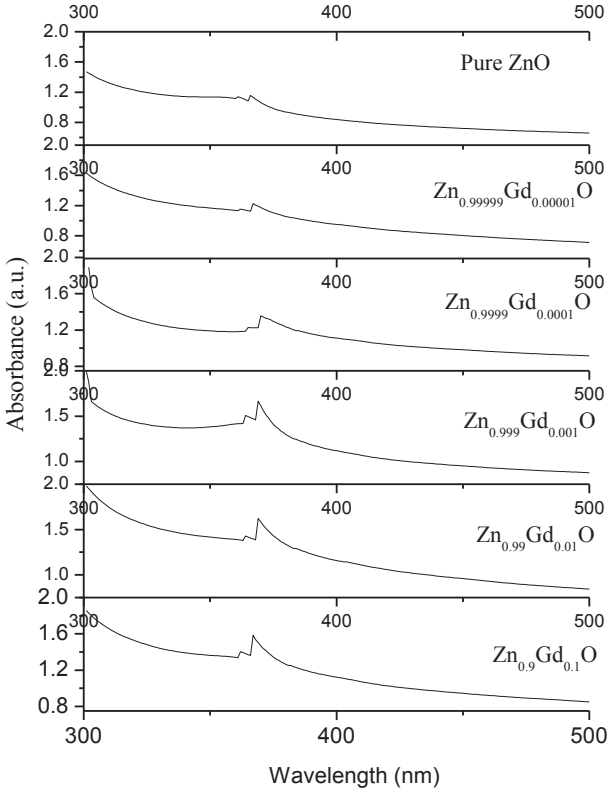

Fig. 5. Absorbance spectra of PVP capped ZnO and $Zn_{1-x}Gd_xO$ ($0.00001 \leq x \leq 0.1$) nanoparticles.

0.00100, 0.00010, 0.00001 and 0.00000, respectively. This data is used to determine the band gap energy of pure and Gd-doped ZnO nanoparticles using the equation (6).

$$E_{bg} = \frac{hc}{\lambda} \tag{6}$$

where E_{bg} is the band gap energy, h is Planck's constant (4.135667×10^{-15} eV s), c is the velocity of light (2.997924×10^{8} m/s), and λ is the absorption wavelength (nm). The value of the band gap obtained for $Zn_{1-x}Gd_xO$ ($0.000001 \leq x \leq 0.1$) nanoparticles are 3.38 eV, 3.36 eV, 3.36 eV, 3.35 eV, 3.38 eV and 3.39 eV for × = 0.10000, 0.01000, 0.00100, 0.00010, 0.00001 and 0.00000, respectively. As the doping gadolinium ions can produce new electronic levels inside the ZnO band gap, thus supports the decreased band gap energy value upon doping.

3.6. Photocatalytic behavior

MO dye is an aromatic compound with azo group and its molecular formula is $C_{14}H_{14}N_3NaO_3S$. The IUPAC name of methyl orange dye is Sodium4[(4dimethylamino)phenyldiazenyl]benzenesulfonate and colour code number is 13025. It is among the commonly used dyes in textile industry and is a highly toxic chemical. It may cause respiratory, eye and skin irritation. Various textile industries release large amount of MO dyes as colored wastewater in natural water resources that make water toxic and hazardous for aquatic flora and fauna. Degradation of MO dye into harmless compounds using ZnO nanophotocatalysts is a highly efficient and cost effective method [35–37]. The present experiments show the Photocatalytic efficiency of ZnO nanoparticles have enhanced by its doping with gadolinium.

Photocatalytic degradation of methyl orange dye was examined using PVP capped $Zn_{1-x}Gd_xO$ nanostructures under UV irradiation using optical absorption spectroscopy. Although the IR studies have confirmed the presence of acetate groups in pure and Gd-doped ZnO nanoparticles which may reduce the photocatalytic efficiency [38], yet an efficient Photocatalytic degradation of MO dye is observed in the presence of prepared nanoparticles. Absorption spectra of methyl orange dye without nanocatalyst before and after UV radiation exposure is shown Fig. 6a for comparison. Absorption peaks were absorbed at 264 nm and 462 nm, where as absorption peak at 462 nm was used to track the photocatalytic degradation process. Absorption spectra have shown a negligible change even after 2 h irradiation. It clearly indicates that aqueous methyl orange dye solution cannot be easily degraded by UV light. The absorption spectra of methyl orange dye solution mixed with $Zn0._{999900}Gd_{0.000100}O$ Fig. 6b. These results clearly show that aqueous methyl orange solution was degraded by the addition of $Zn_{1-x}Gd_xO$ nanophotocatalyst. Fig. 7a and b represents the plots of dye concentration versus the UV irradiation time (t) and plots of $\ln(C_0/C_t)$ versus the UV irradiation time (t) respectively for pure and Gd-doped ZnO nanopowders. Plots of $\ln(C_0/C_t)$ versus the UV irradiation time (t) suggest that the photodegradation of methyl orange dye follows the pseudo-first order kinetics. The values of first-order rate constants (k)

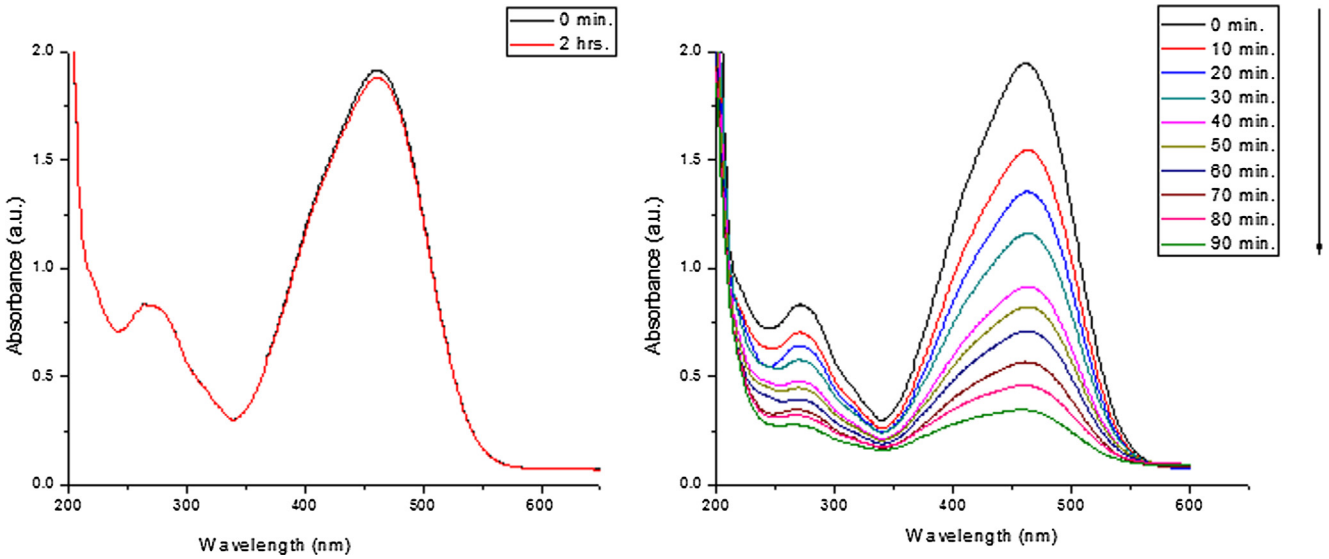

Fig. 6. Ultraviolet–visible spectra of the methyl orange dye in aqueous solution upon irradiation with ultraviolet light in the (a) absence of photocatalyst (b) presence of $Zn_{0.9999}Gd_{0.0001}O$ nanocrystals. (For interpretation of the references to colour in this figure legend, the reader is referred to the web version of this article.)

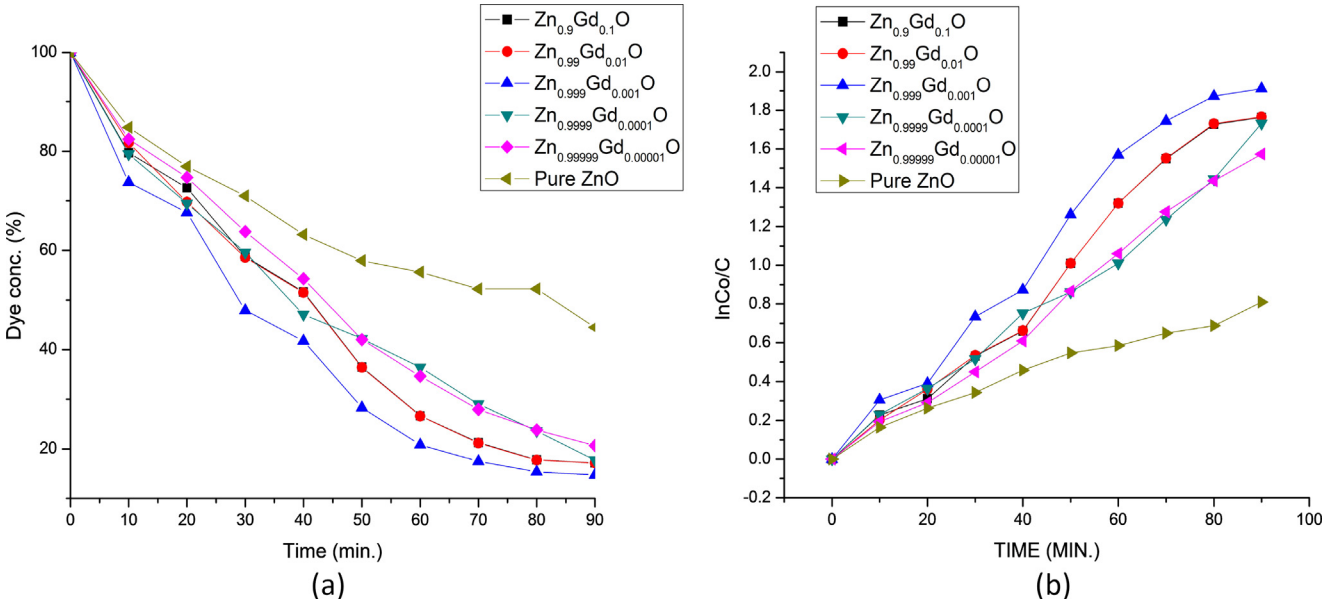

Fig. 7. (a) plots of dye concentration versus the UV irradiation time (t) (b) plots of ln(C0/Ct) versus the UV irradiation time (t).

are 1.96 × 10^{-2} min^{-1}, 1.96 × 10^{-2} min^{-1}, 2.12 × 10^{-2} min^{-1}, 1.92 × 10^{-2} min^{-1}, 1.75 × 10^{-2} min^{-1} and 0.9 × 10^{-2} min^{-1} where as the degradation efficiency (ε) values are 82.83%, 82.89%, 85.30%, 82.30%, 79.33% and 55.50% for various $Zn_{1-x}Gd_xO$ nanoparticles with × = 0.10000, 0.01000, 0.00100, 0.00010, 0.00001 and 0.00000, respectively. The photocatalytic performance is directly proportional to the value of apparent rate constants (k) calculated from the linear fitted curves using Eq. (4). After comparing the values of k, it can be stated that the doping of ZnO with gadolinium has significantly increased its photocatalytic efficiency. Among various doped Zn O nanomaterials, the increasing order The maximum increase is noted in case of $Zn_{0.99900}Gd_{0.00100}O$ nanocrystals (ε = 85.3% and k = 2.12 × 10^{-2} min^{-1}) whereas it is minimum in case of $Zn0._{99999}Gd_{0.00001}O$ nanocrystals (ε = 79.3% and k = 1.75 × 10^{-2} min^{-1}).

Photocatalytic degradation scheme of MO dye under UV light irradiation in the presence of Gd-doped ZnO nanoparticles occurs by following proposed mechanism:

Step I: Absorption of light by Gd doped ZnO nanoparticles that excite electron from valence band to conduction band thus creating a positive hole in valence band.

Step II: Positive holes react with hydroxyl ions produced by ionization of chemisorbed water molecules to produce $O\dot{H}$ radicals, whereas electrons in conduction band reduce oxygen to form superoxide radical $\dot{O_2}$.

Step III: $O\dot{H}$ radicals, being strong oxidizing agents, react with organic dye molecules to cause their complete degradation. The complete mineralization of MO molecule is indicated by decolorization of its intense orange colored aqueous solution and it undergoes demethylation, oxidation and hydroxylation process results in the formation of inorganic products such as SO_4^{2-} ions, NO_3^- ions, CO_2 and H_2O.

The photocatalytic activity of photocatalysts largely depends upon the reducing tendency of electron hole recombination. Presence of various intrinsic and extrinsic defects in such compounds has significantly increased the separation time for electron hole recombination. Intrinsic defects namely oxygen vacancies are the characteristic features of ZnO nanoparticles. Talking about extrinsic defects, doping of ZnO with Gd allows entry of Gd^{3+} into the crystal lattice of ZnO thus creating Zn^{2+} vacancy defects. These extrinsic and intrinsic defects in Gd doped ZnO nanostructures together retard the electron hole recombination time and inturn the photocatalytic efficiency of nanoparticles towards the degradation of methyl orange dye has increased.

4. Conclusions

Bottom up Chemical co-precipitation technique has been successfully employed for the synthesis of pure and Gd-doped ZnO nanoparticles. The insertion of Gd into ZnO has been confirmed from EDXRF studies, while the nanosize wurtzite structure has been revealed from XRD studies. Photocatalytic degradation of methyl orange dye has studied under UV irradiation in the presence of prepared nanoparticles. It suggests that the catalytic efficiency of ZnO photocatalyst have enhanced upon doping with Gadolinium.

Credit author statement

It is a single author paper. All the work is done by author alone.

Declaration of Competing Interest

The authors declare that they have no known competing financial interests or personal relationships that could have appeared to influence the work reported in this paper.

Acknowledgements

I am thankful to the UGC, New Delhi, India, for financial support under College for Potential and Excellence research grant. I acknowledge the guidance and support provided by Dr. Dharminder Singh Ubha, Principal, G.S.S.D.G.S. Khalsa College, Patiala. I am also thankful to Dr. Narinder Singh, Associate Professor, I.I.T., Ropar, Punjab for using his laboratory facilities.

References

[1] M.A. Rauf, I. Shehadeh, A. Ahmed, A. Al-Zamly, J. Int. Chem., Mol. Nuc. Mater. Metallurg. Eng. 3 (7) (2009) 369–374.
[2] M. Catanho, G.R.P. Malpass, A.J. Motheo, Quimica Nova 29 (2006) 983–989.
[3] M. Faisal, M.A. Tariq, M. Muneer, Dyes Pigm 72 (2007) 233–239.
[4] R.J. Kant, Nat Sci. 4 (2012) 22–26.
[5] T. Zhang, T. Oyama, S. Horikoshi, H. Hidaka, J. Zhao, N. Serpone, Solar Ener. Mater. Solar Cells 73 (3) (2002) 287–303.
[6] Sobczyński, A., and Dobosz, A. Polish J. Environ. Studies, 2001, 10(4), 195–205.
[7] T.M. Elmorsi, Y.M. Riyad, Z.H. Mohamed, H.M.H. Abid, E. Bary, J. Hazard. Mater. 174 (2010) 352–356.
[8] S. Gul, O. Ozcan Yildlrln, Chem. Eng. J. 155 (2009) 684–690.
[9] F.H. AlHamedi, M.A. Rauf, S.S. Asraf, Desalination 239 (2009) 159–166.
[10] R. Wahab, S.K. Tripathy, H.S. Shin, M. Mohapatra, J. Musarrat, A.A.A. Khedhairy, N.K. Kaushik, Chem. Eng. J. 226 (2013) 154–160.
[11] S.K. Kansal, A.H. Ali, S. Kapoor, Desalination 259 (1–3) (2010) 147–155.

[12] A. Kajbafvala, H. Ghorbani, A. Paravar, J.P. Samberg, E. Kajbafvala, S.K. Sadrnezhaad, Superlattice Microst. 51 (4) (2012) 512–522.
[13] P.K. Chen, G.J. Lee, S.H. Davies, S.J. Masten, R. Amutha, J.J. Wu, Mater. Res. Bull. 48 (6) (2013) 2375–2382.
[14] L. Xu, Z. Li, Q. Cai, H. Wang, H. Gao, W. Lv, J. Liu, Cryst. Eng. Comm. 12 (2010) 2166–2172.
[15] A. Senthilraja, B. Subash, B. Krishnakumar, D. Rajamanickam, M. Swami-nathan, M. Shanthi, Mater. Sci. Semicond. Process. 22 (2014) 83–91.
[16] H. Wu, W. Pan, J. Am. Ceram. Soc 89 (2006) 699–701.
[17] C.A.K. Gouvea, F. Wypych, S.G. Moraes, N. Duran, P. Peralta-Zamor, Chemosphere 40 (4) (2000) 427–432.
[18] N. Elamin, A. Elsanousi, J. App. Indust. Sci. 1 (2013) 32–35.
[19] Q. Xiao, L.J. Ouyang, Alloy. Compd. 479 (1–2) (2009) 4–7.
[20] J. Zhi-gang, P. Kuan-kuan, L.I. Yan-hua, Z. Rongsun, Trans. Nonferrous Met. Soc. China 12 (2012) 873–878.
[21] S. Ekambaram, Y. Iikubo, A.J. Kudo, Alloy. Compd. 433 (1–2) (2007) 237–240.
[22] F. Min, Y. Li, W. Siwei, L. Peng, J. Liu, F. Dong, Appl. Surf. Sci. 258 (4) (2011) 1587–1591.
[23] M.M.B. Abbad, A.A.H. Kadhum, A.B. Mohamad, M.S. Takriff, K. Sopian, Chemosphere 91 (11) (2013) 1604–1611.
[24] V. Vaiano, M. Matarangolo, O. Sacco, D. Sannino, Chem. Eng. Trans. 57 (2017) 625–630.
[25] U. Alam, A. Khan, D. Ali, D. Bahnemann, M. Muneer, RSC Adv. 8 (2018) 17582–17594.
[26] C. Jun-Lian, D. Neena, L. Na, F. De-Jun, K. Xian-Wen, Chin. Phys. B 27 (8) (2018) 086102.
[27] Hu, B., Sun, Q., Zuo, C., Pei, Y., Yang, S., Zheng, H., Liu, F. Beilstein J. Nanotechnol., 2019, 10, 1157–1165.
[28] H. Parangusan, D. Ponnamma, M.A.A. Al-maadeed, Bull. Mater. Sci. 42 (2019) 179.
[29] A. Samanta, M.N. Goswami, P.K. Mahapatra, Mater. Res. Express 6 (2019) 065031.
[30] P. Pascariu, C. Cojocaru, N. Olaru, P. Samoila, A. Airinei, M. Ignat, L. Sacarescu, D.J. Timpu, Environ. Manage. 239 (2019) 225–234.
[31] K.J. Laidler, J.H. Meiser, ISBN 0-8053-5682-7, Phys. Chem. (1982) 780.
[32] Joint Committee on Powder Diffraction Standards (JCPDS) File No. 05-0664.
[33] V. Rajendar, T. Dayakar, K. Shobhan, I. Srikanth, K.V. Rao, Superlatt. Microstruc. 75 (2014) 551–563.
[34] C.N.R. Rao, Chemical Applications of Infrared spectroscopy, Academic Press, New York and London, 1963.
[35] M.I.H. Chowdhury, M.S. Hossain, M.A.S. Azad, M.Z. Islam, M.A. Dewan, IJSER 9 (6) (2018) 1646–1649.
[36] X. Chen, Z. Wu, D. Liu, Z. Gao, Nanoscale Res Lett 12 (2017) 143.
[37] L.A. Ghule, A.A. Patil, K.B. Sapnar, S.D. Dhole, K.M. Garadkar, Toxicol. Environ. Chem. 93 (4) (2011) 623–634.
[38] T.R. Giraldi, G.V.F. Santos, V.R. Mendonça, C. Ribeiro, I.T. Weber, J. Nanosci. Nanotechnol. 11 (4) (2011) 43635–43640.